J2.3 A FORECASTER-COMPUTER INTERACTIVE CAPABILITY OF THE NCAR AUTO-NOWCASTER SYSTEM FOR IMPROVED STORM INITIATION NOWCASTS

Rita Roberts*, Thomas Saxen, Cynthia Mueller, and David Albo
National Center for Atmospheric Research[1], Boulder CO

1. IMPROVING STORM INITIATION NOWCASTS

A key component and unique attribute of the NCAR Convective Storm Nowcast System (commonly referred to as the Auto-Nowcaster or ANC system; Mueller et al. 2003) is its ability to produce storm initiation nowcasts based on automated radar detections of surface convergence boundaries and characterization of the boundaries (e.g., estimation of shear profiles and maximum vertical velocities along the boundary). Initially designed to run over a single radar domain, the ANC was modified last summer for the Federal Aviation Administration's Regional Convective Weather Forecast (RCWF) demonstration to run over a much larger domain and utilize information from up to four WSR-88Ds. Running the ANC on a larger domain resulted in a deficiency in the ability to detect every boundary present on the local to the synoptic scale. For example, cold fronts evident on synoptic maps were not always well resolved as distinct features on one or more radars.

A new capability has been added to the ANC that allows a forecaster to insert in realtime the locations of convergence features that are not detected or are only partially detected by radar(s). The forecaster-entered boundary locations are then immediately included in all of the boundary characterization algorithms running in the real-time ANC system and directly affect the storm initiation, growth and decay nowcasts produced. This forecaster-computer capability is described here. With the use of this new interactive tool it will now be possible to address the importance of different scale interactions on convection initiation and incorporate these scales in automated nowcasts of storm initiation.

2. FORECASTER-COMPUTER METHODOLOGY

The ANC system includes an automated boundary detection algorithm that identifies boundaries on radar and extrapolates their positions into the future. Boundary detection algorithms have historically used only single Doppler radar data as input and generally have difficulty detecting convergence boundaries that span the distance between two or more radars due lack of overlapping or continuous low-level, clear air return between the radars. Yet these mesoscale features are important triggering mechanisms for convection initiation. Thus, the primary display tool for the ANC system has been modified to allow the forecaster to diagnose and enter the locations of convergence features that extend beyond a single radar domain or may not even be detected by radar. It is anticipated that having a forecaster periodically enter convergence boundary locations, particularly those on the synoptic and mesoscale, will improve 0-2 hr nowcasts of storm initiation.

2.1 Forecaster Use of the Diagnostic Tool

One advantage of having a forecaster in the loop is that he can make use of several other data sets in addition to mosaic radar data to identify convergence boundaries. These data sets include: numerical model output (RUC-20km), satellite imagery, numerical boundary layer model wind field and surface mesonet data. The strategy used to define and enter boundaries is documented below using data from an RCWF case on 20 May 2003.

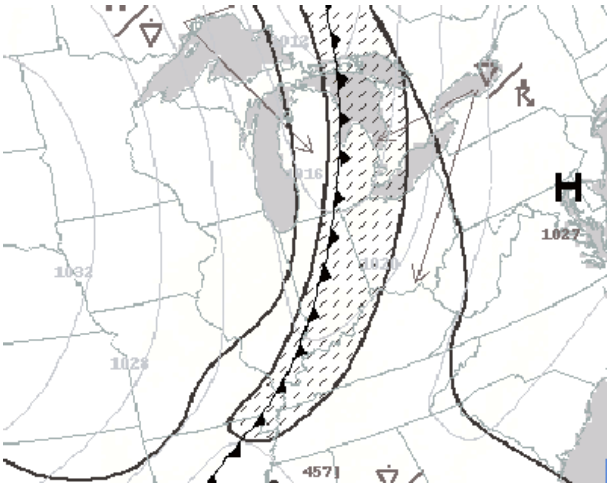

Figure 1. Forecast map of fronts, pressure and weather issued by NOAA/NCEP/HPC, valid at 1200 UTC on 20 May 2003.

At the start of the day, the forecaster looks at the numerical model forecasts to anticipate the weather activity during the day. On 20 May, a cold front (see Fig. 1) was expected to pass through the RCWF domain that includes portions of Illinois, and Ohio and most of Indiana. In Fig. 2, a selection of the datasets available to the forecaster for viewing the large scale attributes of the atmosphere using the ANC system are shown. These particular datasets are used by the forecaster for defining and entering convergence boundaries. In Fig. 2a, at 1600 UTC, the low-level RUC wind field is overlaid onto a derived frontal likelihood field. The frontal likelihood

*Corresponding author address: Rita Roberts, NCAR, P.O. Box 3000, Boulder, CO 80307, email: rroberts@ucar.edu

[1]NCAR is sponsored by the National Science Foundation

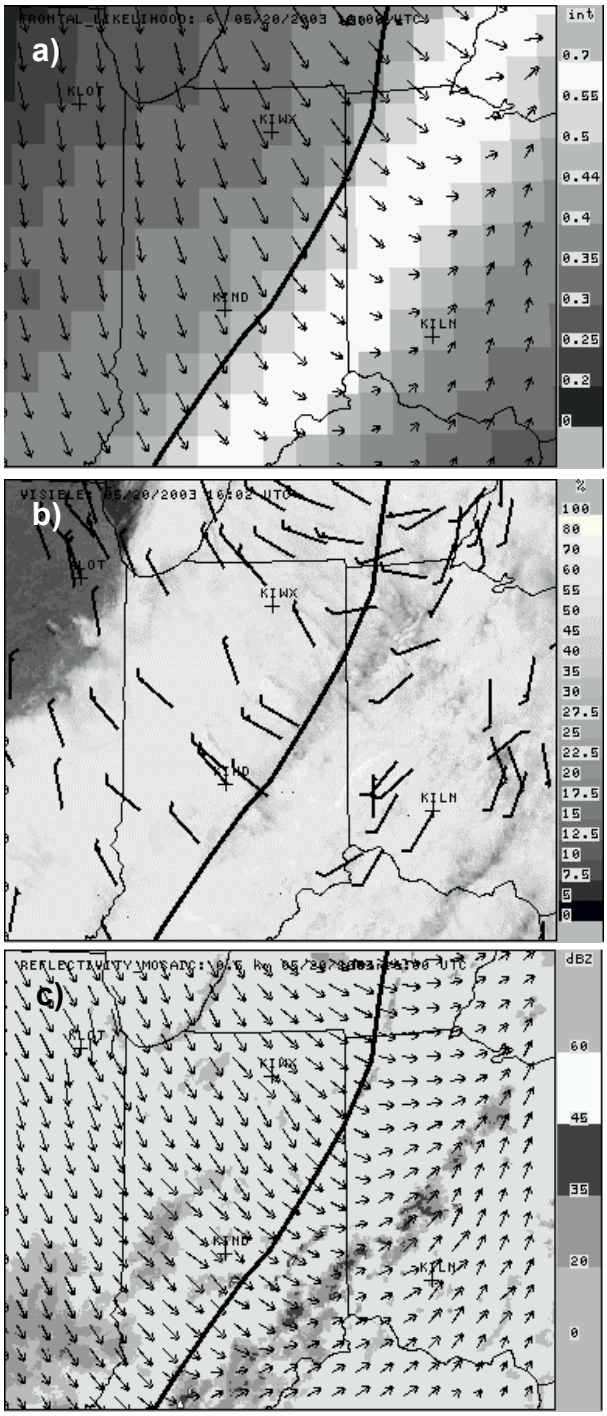

Figure 2. Data used by the forecaster to enter convergence boundary locations (solid black line) on 20 May 2003 at 1600 UTC. a) RUC low-level winds overlaid onto a RUC-based frontal likelihood field. b) GOES visible satellite image with ASOS and AWOS station data overlaid. c) Mosaic radar reflectivity at 0.5 km with VDRAS boundary layer winds at 0.187 km overlaid.

field is produced from a feature detection algorithm that automatically defines broad zones of frontal locations based on a combination of weighted, RUC-derived convergence, equivalent potential temperature gradient and vertical vorticity fields (Mueller and Megenhardt, 2003). The lighter gray and white regions in Fig. 2a define the current position of the large scale frontal zone as it extends through portions of Indiana and Ohio. Most of the domain was covered by widespread cloudiness associated with the cold front (Fig. 2b). So the satellite data was not particularly useful for identifying lines of new convective growth resulting from converging winds or from thunderstorm outflows in the boundary layer. In contrast, the METAR data in Fig. 2b was quite useful providing information on the location, movement and intensity of the front throughout the afternoon.

Two additional fields important for monitoring change in convective activity are the mosaic radar reflectivity field that provides information on storm development and evolution and the numerical boundary layer wind fields produced by the four-dimensional, variational Dopper radar analysis system (VDRAS; Sun and Crook, 2001) shown in Fig. 2c. VDRAS is able to provide real-time winds every 12 minutes on a high resolution grid with 4 km spacing and at 1600 shows the change in wind direction and speed associated with the approaching front. The NE-SW lines of radar echoes located ahead of the front are weak to moderate storms that have tracked eastward through the area since early morning.

Because of the broad extension of the cold frontal boundary, the automated boundary detection algorithm was unable to detect any significant shear or clear-air reflectivity thin lines associated with this front in any of the WSR-88D radar datasets within the RCWF domain. Thus, the forecaster used the datasets illustrated in Fig. 2 to enter the location of the cold front at two different time periods in order to obtain the motion of the boundary with time. This motion vector is used in producing the 60 min extrapolated position of the boundary (solid black line) as shown in Fig. 2 at 1600.

2.2 Computer Processing of Forecaster-entered Boundaries

At 1655 UTC in Fig. 3a, very little has changed in the VDRAS winds patterns and most of the storms to the east have maximum reflectivity intensities of < 35 dBZ. None of the available data exhibited an intensification of the convergence along the front or the presence of a gust front within the domain that could trigger convection. Thus the forecaster decides that updated location of the cold frontal boundary does not need to be entered. An enhancement to the ANC automated boundary detection algorithm enables the algorithm to continue to ingest the forecaster-entered boundary (and associated boundary motion) at 1600, propagate its position with time, produce updated 60 min extrapolation positions every 6 min and automatically display these new positions on the ANC display.

One hour later (Fig. 3b) at 1755, a change has occurred in the environment leading to development of >40 dBZ storms along the northern and southern portions of the cold front. These storms develop in spite of the fact that there has been little change in the character-

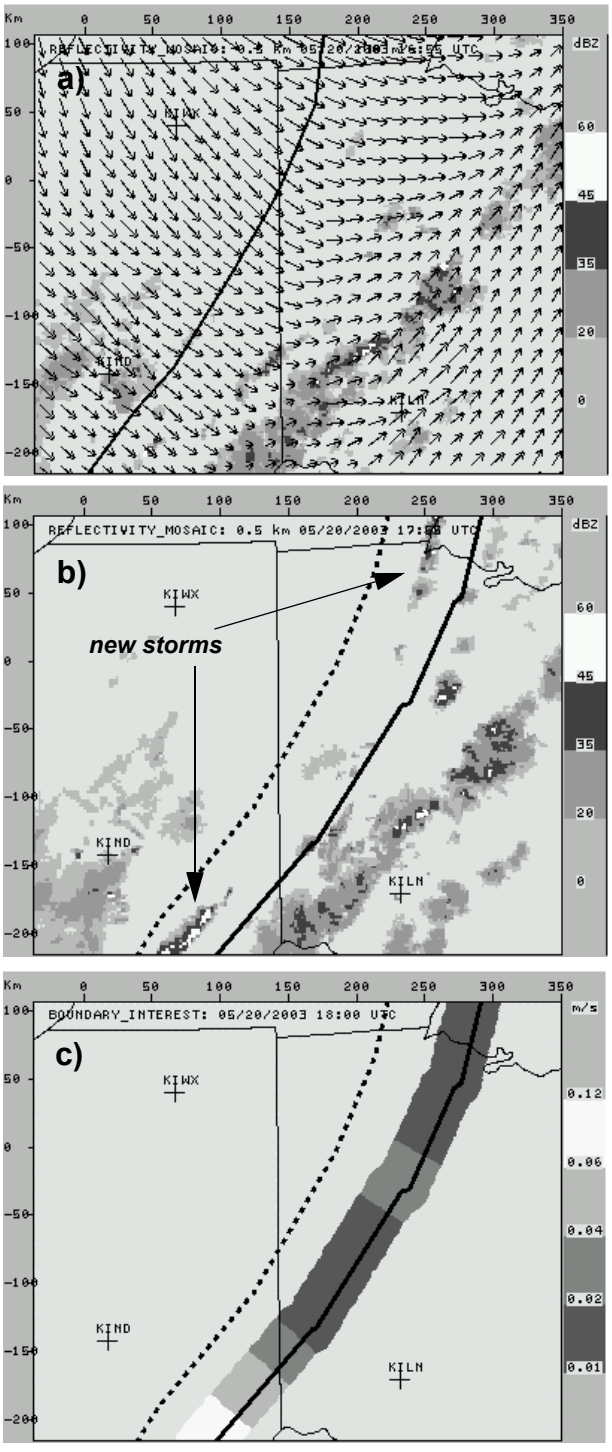

Figure 3. The forecaster-computer process. a) VDRAS winds at 0.187 km AGL overlaid onto the reflectivity mosaic field at 1655 UTC. Solid black line is the 60 min extrapolated position of the forecaster-entered boundary. b) Reflectivity mosaic field at 1755 UTC with the new forecaster-entered boundary (dashed line) and corresponding, computer-derived 60 min extrapolated position (solid line) overlaid. c) One of the boundary interest fields produced from the boundary characterization algorithm that ingested the boundaries shown in (b) and are also overlaid here.

istics and convergence magnitudes of the cold frontal boundary and in the RUC-based stability fields (Trier et al, 2002). The forecaster, realizing this change has occurred, enters a revised location for the cold front (dashed line in Fig. 3b) and increases the weights for this area in the ANC system based on the new convection that has occurred.

Once the forecaster has entered the new boundary location on the display, the automated boundary detection algorithm produces a 60 min extrapolation position (solid line in Fig. 3b). This extrapolation position is then read into the ANC boundary characterization algorithms that determine the boundary speed, the low-level shear, the boundary-relative steering flow (i.e., likelihood of storms to remain colocated with the boundary), maximum vertical velocity, and the occurrence of past storm initiations along the boundaries. Figure 3c shows one of the boundary interest fields produced 5 min after the boundary is ingested into the ANC. The lighter gray shades represent regions of higher interest for storm initiation and growth. This interest field is then combined in the ANC with other boundary, cloud and storm-related information to produce 60 min storm initiation, growth and decay nowcasts issued every 6 min (Mueller et al. 2003). Note that the ANC nowcasts are location-specific for > 35 dBZ storms.

3. STORM INITIATION NOWCASTS

As mentioned previously the radar-based, automated boundary detection algorithm did not identify any convergence regions in the KILN, KIND, KIWX and KLOT WSR-88D data associated with the cold front. Figure 4a illustrates the 60 min nowcasts at 1856 that would have been produced if no boundaries had been entered by the forecaster. The nowcasted storm locations shown in Fig. 4a are primarily based on extrapolation of existing storms.

Figure 4b shows the 60min nowcasts produced when the forecaster-entered boundary locations at 1755 were included in the ANC. In addition to the extrapolation of existing storms, a storm initiation zone (shaded, rectangular region) is nowcast along the cold front, defining the region where new storms are expected to develop in 60 min. Existing storm already present within the initiation zone are expected to intensify over the next 60 min.

Verification data from 1955 is overlaid onto the nowcasts issued at 1856 in Fig. 4c. It is evident that a whole new line of convection developed within the initiation zone and that most of the existing (extrapolated) storms did indeed persist 60 min later. It is clear that the forecaster-entered boundaries enabled significant increase in performance in the 60 min nowcasts.

4. SUMMARY

A new tool for entering convergence boundaries into the ANC has been tested and is being used during the real-time RCWF 2003 demonstration being conducted in the NE portion of the U.S. Forecasters can enter both large scale features such as frontal zones that are gener-

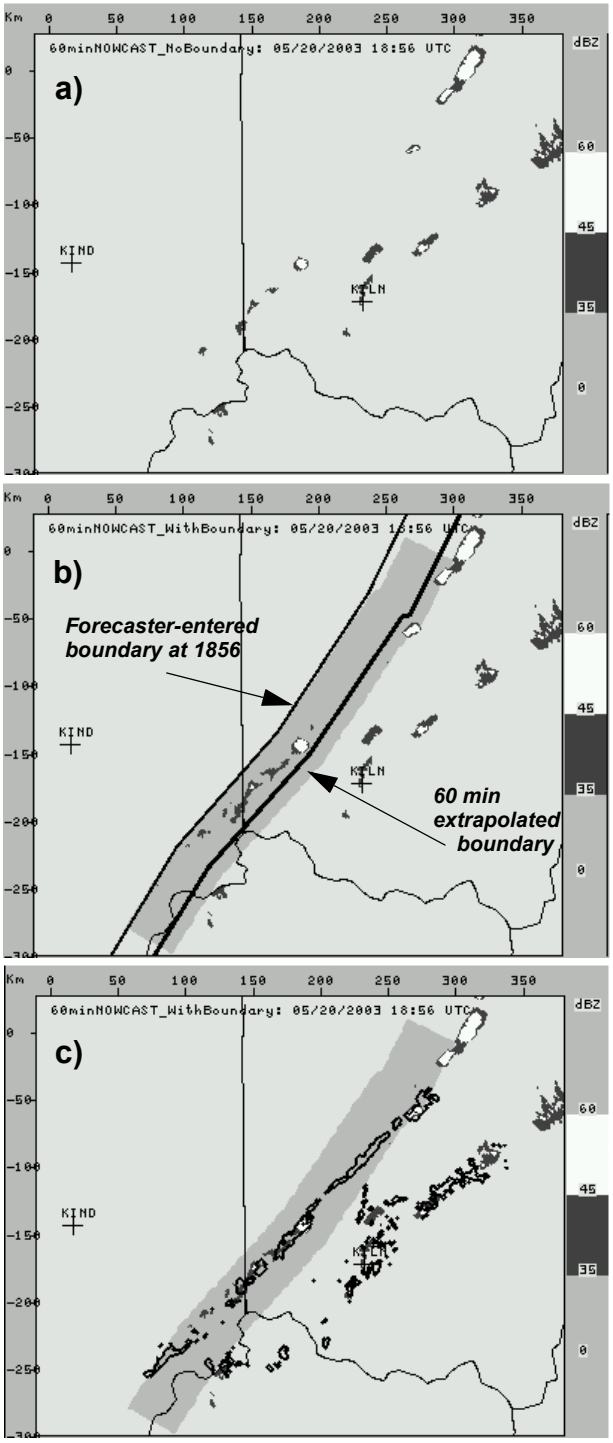

Figure 4. Storm initiation nowcasts issued at 1856 UTC with radar reflectivity echoes > 30 dBZ overlaid. a) 60 min nowcast produced without forecaster input. Echoes shown are the 60 min extrapolated positions of storms at 1856 expected to persist until 1955 UTC. b) 60 min nowcast produced with the forecaster-entered boundary (solid lines) included in the ANC system. The shaded, rectangular area defines the storm initiation zone where new storms are expected to be located in 60 min. Echoes outside the zone are as in (a). c) Same as in (b) but with contours of radar reflectivity > 30 dBZ from 1955 overlaid.

ally easy to identify in the data and smaller scale thunderstorm outflow locations. The interface between the display tool and ANC algorithms was designed in such a way that it takes very little of the forecaster's time, only a few minutes at most, to add these features into the system. In addition, it is generally unnecessary for the forecaster to insert a convergence boundary location more than once every 1-2 h, unless the motion of the boundary changes significantly during a specific time period. In the event that this occurs, the forecaster would likely want to enter an updated boundary position so that the change in boundary motion would be accurately represented in producing the 60 min boundary extrapolation.

Having the forecaster in the loop has been shown here to have a tremendous impact on the performance of the nowcasting system. The additional information the forecaster provides on boundary locations can make a significant difference in the nowcast accuracy due to the very important effects these features have on storm initiation and growth.

References

Mueller, C., and D. Megenhardt, 2003: Predictability of storm characteristics based on RUC environmental fields. *Preprints, 31st Conf. on Radar Meteor.*, AMS, Seattle, this preprint volume.

Mueller, C.K., T. Saxen, R. Roberts, J. Wilson, T. Betancourt, S. Dettling, N. Oien, and J. Yee, 2003: NCAR Convective Storm Nowcasting System. *Wea. Forecasting,* **18**.

Sun, J. and N.A. Crook, 2001: Real-time low-level wind and temperature analysis using single WSR-88D data. *Wea. Forecasting*, **16**, 117-132.

Trier, S., D. Ahijevych, C. Davis, D. Megenhardt, C. Mueller, and N. Rehak, 2002: Enhancement of 0-3h forecasts of deep convection using mesoscale diagnostics derived from operational model analyses and forecasts. *International Conf. on Quantitative Precipitation Forecasting*, Reading, UK.